ON SOLUTE TRANSPORT IN OSCILLATORY FLOW THROUGH AN ANNULAR PIPE WITH A REACTIVE WALL AND ITS APPLICATION TO A CATHETERIZED ARTERY

by B. S. MAZUMDER *and* KAJAL KUMAR MONDAL

(*Physics and Applied Mathematics Unit, Indian Statistical Institute, Kolkata* 700 108, *India*)

[Received 19 December 2002. Revises 23 April and 25 November 2004]

Summary

Longitudinal dispersion of passive tracer molecules released in a pulsatile flow through an annular pipe with a reactive outer wall is studied by employing the method of integral moments. It is shown how the spreading of tracers is influenced by the shear flow due to a periodic pressure pulsation in the pipe and a first-order reaction at the wall. The behaviour of the dispersion coefficient due to variation of the aspect ratio (the ratio of the inner radius to the outer radius of the annular pipe) for periodic flow with and without a non-zero mean is examined. It is shown that an increase of aspect ratio, Womersley parameter or reaction at the outer wall of the annular pipe inhibits the dispersion of tracers. The axial distribution of the mean concentration is approximated using a Hermite polynomial representation from the first four central moments for a range of different aspect ratios and frequencies of the pressure pulsation. It is interesting to note that for low frequencies of pulsation, an increase of aspect ratio leads to a significant effect on the concentration distribution, whereas for large frequencies, this effect tends to diminish. The results of this study are of great importance in understanding the dispersion process in a catheterized artery with a reactive arterial wall.

1. Introduction

The study of longitudinal dispersion of a tracer in a straight tube has a wide range of applications in the fields of chemical, environmental and biomedical engineering. The dispersion of diffusing solute in a fluid flowing through a circular impermeable tube was first described by Taylor (**1**) and subsequently extended by Aris (**2**) for pipe Poiseuille flow using the method of moments. They confirmed that after a sufficiently long time when the tracer was completely mixed across the tube, any localized initial configuration of the tracer material evolved to a Gaussian distribution moving with the mean speed of the flow. Using his method of moments, Aris (**3**) analysed the longitudinal dispersion of solute in an oscillatory flow of a viscous incompressible fluid under a periodic pressure gradient. However, his analysis of the dispersion coefficient was restricted to asymptotically large times after the injection of the solute. Watson (**4**) studied the mass transfer of a diffusing substance in oscillatory flow through a pipe. Grotberg (**5**) analysed oscillatory viscous flow in a tapered channel under conditions of fixed Stokes volume by developing a lubrication theory and Gaver and Grotberg (**6**) verified experimentally that both theoretical and experimental results show a bi-directional drift for all frequencies depending on the value of the Womersley parameter. Rao and Deshikachar (**7**) explored the generalized dispersion model proposed by Gill and Sankarasubramanian (**8**) to study the dispersion of a diffusing solute in an annular pipe and evaluated the dispersion coefficient for

all times. Pedley and Kamm (**9**) studied the axial mass transport in an annular region by asymptotic analysis for the limiting case of small annular gap and by numerical solution for arbitrary annular gap in a curved tube in the presence of an oscillatory flow field. Since the pioneering work of Taylor (**1**), dispersion problems have been studied for a great variety of transport problems by Chatwin (**10**), Jimenez and Sullivan (**11**), Mukherjee and Mazumder (**12**), Hydon and Pedley (**13**) and others, but dispersion with boundary absorption in an annular pipe has not received much attention despite the fact that it is of great importance in environmental and physiological fluid dynamics.

Smith (**14**) used a delay-diffusion equation to study the effect of boundary reaction on longitudinal dispersion in shear flows. Purnama (**15**) investigated the case of reaction and retention at the flow boundaries when the tracer is chemically active. Mazumder and Das (**16**) and Jiang and Grotberg (**17**) studied the effect of wall conductance on the axial dispersion of solute in oscillatory tube flow and found that the frequency parameter and wall permeability play important roles in the transport of the solute concentration. Jayaraman *et al.* (**18**) analysed solute transport in a fluid flowing within a curved tube with absorbing wall. Their results, based on perturbation and spectral methods, confirmed that the influence of secondary flows on dispersion is reduced if the tracer is heavily soluble in the wall.

Pulmonary artery catheterization is now extensively used in medical science for the measurement of various physiological flow characteristics as well as for the diagnosis and treatment of various arterial diseases (**19, 20**). Jayaraman and Tiwari (**21**) showed that catheterization in a curved artery leads to an increase in the axial wall shear stress. Dash *et al.* (**22**) studied the Casson model to understand the flow pattern for both steady and unsteady flows in a catheterized artery. Recently, Sarkar and Jayaraman (**23**) analysed pulsatile blood flow through a catheterized artery with an elastic outer wall.

The main purpose of the present paper is to explore the combined effects of aspect ratio, frequency of pressure pulsation and first-order heterogeneous chemical reaction at the outer wall on the streamwise dispersion of tracer material released in a pulsatile flow through an annular pipe. More precisely, results are obtained numerically for the time evolution of the flow, showing how the spreading of tracers is influenced by the shear flow caused by a periodic pressure gradient with and without a non-zero mean, how the tracer molecules are depleted or protected by boundary reaction, how the centre of mass moves, and what patterns of axial mean concentration evolve in the presence of reaction at the wall. The axial distribution of concentration is approximated by using a Hermite polynomial representation. The solute is initially uniform over the cross-section of the annular pipe and the Péclet number is large. The work is significant in the analysis of dispersion through a catheterized artery in the presence of a boundary reaction and the results may allow a correction to be made for the catheter-induced error based on the longitudinal dispersion of tracers by the combined action of convection, diffusion and reaction.

2. Mathematical formulation

Consider an unsteady fully developed viscous, incompressible, axisymmetric pulsatile laminar flow through an annular pipe (Fig. 1). The length of the pipe is assumed to be large enough compared to its diameter that entry effects can be neglected. The radial and axial coordinates are r^* and z^* respectively, where the asterisk denotes dimensional quantities. The flow is driven by a periodic axial pressure gradient with a non-zero mean given by

$$-\frac{1}{\varrho}\frac{\partial p}{\partial z^*} = P_{z^*}(1 + \varepsilon e^{i\omega^* t^*}), \tag{1}$$

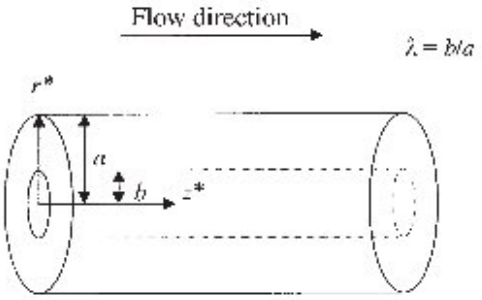

Fig. 1 Schematic diagram of an annular pipe

where ϱ is the density of the homogeneous fluid, P_{z^*} is the mean pressure gradient and ε and ω^* are the amplitude and frequency of the pressure pulsation. The axial velocity $u^*(r^*, t^*)$ satisfies the Navier–Stokes equation

$$\frac{\partial u^*}{\partial t^*} = -\frac{1}{\varrho}\frac{\partial p}{\partial z^*} + \nu \frac{1}{r^*}\frac{\partial}{\partial r^*}\left(r^*\frac{\partial u^*}{\partial r^*}\right) \tag{2}$$

with no slip conditions at both walls of the annular pipe, that is, $u^*(r^*, t^*) = 0$ at $r^* = a$ and $r^* = b$, and where ν is the kinematic viscosity of the fluid. When a passive solute of constant molecular diffusivity D is released into the time-dependent flow, the concentration $C(t, r, z)$ of the solute satisfies the non-dimensional convective-diffusion equation

$$\frac{\partial C}{\partial t} + \mathrm{Pe}\, u(r,t)\frac{\partial C}{\partial z} = \frac{1}{r}\frac{\partial}{\partial r}\left(r\frac{\partial C}{\partial r}\right) + \frac{\partial^2 C}{\partial z^2} \tag{3}$$

with dimensionless quantities defined by

$$r = \frac{r^*}{a}, \quad z = \frac{z^*}{a}, \quad t = \frac{Dt^*}{a^2}, \quad u = \frac{u^*}{U}, \quad \mathrm{Pe} = \frac{Ua}{D}.$$

Here $u(r, t)$ is composed of a steady velocity component $u_0(r)$ and a periodic velocity component $u_1(r, t)$ due to the imposed pressure gradient, U is the time averaged axial velocity $(P_{z^*}a^2/4\mu)$ considered as the reference velocity, where μ is the coefficient of viscosity of the fluid and Pe is the Péclet number which measures the characteristic time of the diffusion process $\left(a^2/D\right)$ relative to the convection process (a/U). The initial and boundary conditions are

$$\left.\begin{aligned} &C(0, r, z) = B(r)\delta(z) \quad (\lambda \leqslant r \leqslant 1), \\ &\frac{\partial C}{\partial r} + \beta C = 0 \quad \text{at} \quad r = 1, \\ &\frac{\partial C}{\partial r} = 0 \quad \text{at} \quad r = \lambda, \\ &C \quad \text{finite at all points}, \\ &\frac{1}{1-\lambda}\frac{1}{\pi}\int_\lambda^1 \int_0^{2\pi} \int_{-\infty}^{\infty} rC(0, r, z)\,dr\,d\theta\,dz = 1, \end{aligned}\right\} \tag{4}$$

where $B(r)$ is a specified function of r, δ is the Dirac delta function, $\beta\ (= \beta^* a)$ is the first-order reaction rate or absorption parameter and $\lambda = b/a$ is the ratio of the inner radius b to the outer

radius a of the annular pipe. The final condition in (4) represents the fact that the total amount of material in the annular pipe is taken to be unity at $t = 0$ assuming $B(r) = 1/(1+\lambda)$ for $\lambda \leqslant r \leqslant 1$.

The flow velocity $u(r, t)$ in (3) is obtained from the solution of equations (1) and (2), together with the no-slip conditions $u = 0$ at the walls $r = \lambda, 1$; it is given by

$$u(r, t) = u_0(r) + u_1(r, t), \tag{5}$$

where

$$u_0(r) = \left[1 - r^2 - \frac{1-\lambda^2}{\ln \lambda} \ln r\right], \quad 0 < \lambda < 1, \tag{6}$$

$$u_1(r, t) = \mathrm{Re}\left[\frac{4i\epsilon}{\alpha^2} [F(r) - 1] e^{i\alpha^2 St}\right], \tag{7}$$

and

$$F(r) = \frac{\left[K_0(\lambda\alpha i^{1/2}) - K_0(\alpha i^{1/2})\right] I_0(r\alpha i^{1/2}) + \left[I_0(\alpha i^{1/2}) - I_0(\lambda\alpha i^{1/2})\right] K_0(r\alpha i^{1/2})}{\left[K_0(\lambda\alpha i^{1/2}) I_0(\alpha i^{1/2}) - I_0(\lambda\alpha i^{1/2}) K_0(\alpha i^{1/2})\right]}.$$

Here I_0, K_0 are the modified Bessel functions of first and second kinds of order zero respectively with imaginary arguments (Tsangaris and Athanassiadis (**24**)). The functions I_0 and K_0 can be expressed as $I_0(xi^{1/2}) = \mathrm{ber}(x) + i\,\mathrm{bei}(x)$ and $K_0(xi^{1/2}) = \mathrm{ker}(x) + i\,\mathrm{kei}(x)$, where ber, bei, ker, and kei are Kelvin functions of order zero (Abramowitz and Stegun (**25**)). Also $\alpha = a\sqrt{\omega^*/\nu}$ is the dimensionless frequency parameter or Womersley number which is a function of the product of two dimensionless parameters, the Reynolds number Ua/ν and the Strouhal number $\omega^* a/U$. The parameter α^2 is a measure of the ratio of the time (a^2/ν) required for viscosity to smooth out the transverse variation in vorticity to the time period of the oscillation $(1/\omega^*)$. Another way of looking at α is that, for periodic flow in an annular pipe, it is the ratio of the outer radius a to the thickness of the Stokes boundary layer $\sqrt{\nu/\omega^*}$. Thus we may treat α^2 as a kind of unsteady Reynolds number. The Schmidt number $S(= \nu/D)$ represents the ratio of viscous diffusion to molecular diffusion, and $\alpha^2 S$ is a measure of the ratio of the characteristic time of transverse diffusion to the period of oscillation. When the aspect ratio λ approaches 0, equations (6) and (7) reduce to the flow due to mean and periodic pressure gradients through a circular pipe:

$$u_0(r) = 1 - r^2, \tag{8}$$

$$u_1(r, t) = \mathrm{Re}\left[\frac{4i\epsilon}{\alpha^2} \left[F^*(r) - 1\right] e^{i\alpha^2 St}\right], \tag{9}$$

where

$$F^*(r) = \frac{I_0(r\alpha i^{1/2})}{I_0(\alpha i^{1/2})}.$$

Figure 2 shows the periodic flow (7) in a pipe of annular cross-section for various values of the frequency parameter α, aspect ratio λ, phase difference $\alpha^2 St$ and for $\epsilon = 1$. It is observed that increase of the aspect ratio λ leads to a decrease in the velocity and it approaches a symmetric parabolic profile similar to that for the flow through a pipe. Also, as the frequency parameter α increases, the velocity decreases. Equation (8) corresponds to pipe Poiseuille flow, which leads to

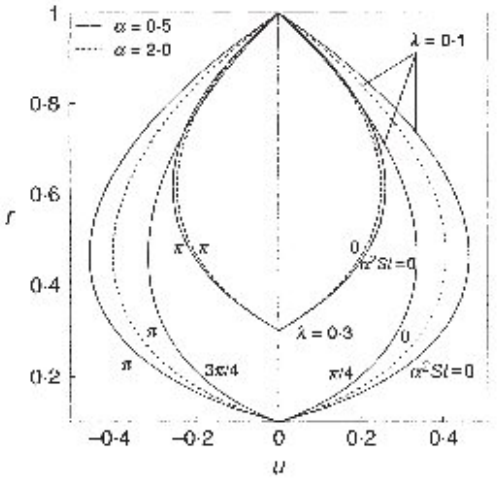

Fig. 2 Velocity profiles for different values of the aspect ratio λ and frequency parameter $\alpha = 0{\cdot}5$ (solid line) and $2{\cdot}0$ (dotted line), for different phases $\alpha^2 St = 0, \pi/4, 3\pi/4, \pi$ for $\lambda = 0{\cdot}1$ and $\alpha^2 St = 0, \pi$ for $\lambda = 0{\cdot}3$

a maximum velocity at the centre-line of the pipe $r = 0$, and equation (9) corresponds to periodic flow through a pipe.

Following the method of integral moments proposed by Aris (**2**), the diffusion equation (3) subject to the initial and boundary conditions can be written as

$$\frac{\partial C_p}{\partial t} - \frac{1}{r}\frac{\partial}{\partial r}\left(r\frac{\partial C_p}{\partial r}\right) = pu(r,t)\mathrm{Pe}\, C_{p-1} + p(p-1)C_{p-2} \tag{10}$$

with

$$\left.\begin{aligned} C_p(0,r) &= \begin{cases} (1+\lambda)B(r) & \text{for } p = 0, \\ 0 & \text{for } p > 0, \end{cases} \\ \frac{\partial C_p}{\partial r} + \beta C_p &= 0 \quad \text{at} \quad r = 1, \\ \frac{\partial C_p}{\partial r} &= 0 \quad \text{at} \quad r = \lambda, \end{aligned}\right\} \tag{11}$$

where it is assumed that $B(r) = 1/(1+\lambda)$ for $\lambda \leqslant r \leqslant 1$, and $C_p(t,r)$ is the pth integral moment of the distribution of tracer in the filament for all z at time t given by

$$C_p(t,r) = \int_{-\infty}^{\infty} z^p C(t,r,z)\,dz. \tag{12}$$

Averaging over the annular cross-section, equations (10) and (11) become

$$\frac{dM_p}{dt} = pPe\,\overline{u(r,t)C_{p-1}} + p(p-1)\overline{C_{p-2}} - \frac{2\beta}{1-\lambda^2}C_p(t,1) \tag{13}$$

and

$$M_p(0) = 1 \quad \text{for} \quad p = 0, \quad M_p(0) = 0 \quad \text{for} \quad p > 0, \tag{14}$$

where an overbar denotes the cross-sectional mean and $M_p(t)$ is the pth moment of the distribution of tracer over the cross-section of the annular pipe,

$$M_p(t) = \bar{C}_p = \frac{\int_0^{2\pi} d\theta \int_\lambda^1 rC_p(t,r)dr}{\int_0^{2\pi} d\theta \int_\lambda^1 rdr}. \tag{15}$$

The pth central moment of the concentration distribution about the mean can be defined as

$$\mu_p(t) = \frac{\frac{1}{1-\lambda}\frac{1}{\pi}\int_\lambda^1 \int_0^{2\pi} \int_{-\infty}^{\infty} r(z-\mu_g)^p C dr d\theta dz}{\frac{1}{1-\lambda}\frac{1}{\pi}\int_\lambda^1 \int_0^{2\pi} \int_{-\infty}^{\infty} rC(0,r,z) dr d\theta dz}, \tag{16}$$

where $\mu_g = M_1/M_0$ is the centroid or first moment of the solute, which measures the location of the centre of gravity of a slug with mean velocity in the annular flow initially located at the source, and M_0 represents the total mass of the reactive solute in the whole volume of the annular pipe. From (16), μ_2 represents the variance related to the dispersion of the tracer about the mean position and the third (μ_3) and fourth (μ_4) central moments represent the skewness and kurtosis of the distribution of the tracer respectively. The variance $\sigma_z^2 = \mu_2$, and the coefficients of skewness (λ_3) and kurtosis (λ_4) are the important criteria for measuring the degree of symmetry and peakedness of the concentration distribution of solute respectively, and are given by

$$\lambda_3 = \frac{\mu_3}{\mu_2^{3/2}} \quad \text{and} \quad \lambda_4 = \frac{\mu_4}{\mu_2^2} - 3. \tag{17}$$

For a Gaussian distribution both λ_3 and λ_4 are zero, and non-zero values of skewness and kurtosis indicate deviations from normality. A negative value of the skewness indicates an asymmetric profile with a tail to the left of the maximum and negative and positive values of λ_4 represent leptokurtic and platykurtic distributions respectively.

3. Numerical solution

Owing to the complexity of the analytical solution of the moment equations ($p \geqslant 1$) subject to the initial and boundary conditions for $\beta \neq 0$ and $\lambda \neq 0$, a finite difference method based on the Crank–Nicolson implicit scheme was adopted to study the problem. The scheme has been discussed in detail in the work of Mazumder and Das (**16**). The derivatives and all other terms are written at the mesh point $(i+1, j)$, where $i = 1$ corresponds to the time $t = 0$ and $j = 1$ to the inner wall of the annular pipe at $r = \lambda$. The mesh point (i, j) indicates a point where $t_i = \Delta t \times (i-1)$ and $r_j = \lambda + (j-1) \times \Delta r$, with Δt and Δr the increments in t and r respectively. The resulting finite difference equation becomes a system of linear algebraic equations with a tri-diagonal coefficient matrix,

$$P_j C_p(i+1, j+1) + Q_j C_p(i+1, j) + R_j C_p(i+1, j-1) = S_j, \tag{18}$$

where P_j, Q_j, R_j and S_j are the matrix elements.

The finite difference forms of the initial and boundary conditions are

$$\left.\begin{aligned} C_p(1, j) &= \begin{cases} 1 & \text{for } p = 0, \\ 0 & \text{for } p > 0, \end{cases} \\ C_p(i+1, 2) &= C_p(i+1, 0) \end{aligned}\right\} \tag{19}$$

at the inner wall, and

$$C_p(i+1, M+1) = C_p(i+1, M-1) - 2\beta \Delta r C_p(i+1, M) \tag{20}$$

at the outer wall of the annular pipe for $p \geqslant 0$, where M is the value of j at the outer wall.

This tri-diagonal coefficient matrix was solved using the Thomas algorithm (Anderson *et al.* (**26**)) with the help of the prescribed initial and boundary conditions. For the periodic flow with or without a non-zero mean, a mesh size $\Delta t = 0{\cdot}00001$, $\Delta r = (1-\lambda)/M$, where λ varies from 0·02 to 0·4 and $M = 31$, gives satisfactory results for values of the frequency parameter $\alpha = 0{\cdot}5$, 1·0, 2·0 and 3·0. In all cases we have taken $\epsilon = 1$.

4. Results and discussion

In order to validate the numerical scheme with the analytical results, a check was made on the statistical properties (mean, variance, skewness and kurtosis) of the concentration distribution an longitudinal dispersion coefficient for the periodic flow with and without a non-zero mean, with th aspect ratio $\lambda = 0$ and in the absence of reaction ($\beta = 0$) at the boundary. The results show good agreement with those of Gill and Sankarasubramanian (**8**), Barton (**27**), Rao and Deshikachar (**7**) for time independent flow, and with Mukherjee and Mazumder (**12**) and Mazumder and Das (**16**) for periodic flow with and without a non-zero mean, so the numerical scheme was then extended to the periodic flow with non-zero mean in an annular pipe with absorbing wall.

It is observed for periodic flow with zero mean that the first moment (μ_g) which measures th centre of gravity of the solute moves cyclically with the same frequency as the oscillatory currer when the frequency parameter α and aspect ratio λ are fixed. The amplitude of the oscillation i creases with the boundary reaction β; that is, the mean displacement of the solute increases wi each complete period of oscillation. When λ increases the centroid displacement of the solute moves in a wavy manner but the amplitude of the oscillation decreases. For periodic flow with non-zero mean, the centroid of the solute moves cyclically with the oscillatory nature of the flow; the amplitude of the oscillation increases with the boundary reaction β and decreases with increase of λ.

According to Aris (**2**), the effective longitudinal dispersion coefficient D_a may be defined as

$$D_a(\alpha, S, \lambda, \epsilon, \beta, t) = \frac{1}{2\mathrm{Pe}^2} \frac{d\sigma_z^2}{dt}, \tag{21}$$

where σ_z^2 is the variance of the longitudinal concentration distribution. If the variance increases linearly with time, the longitudinal dispersion is constant. Here the dispersion coefficient D_a depends on the Womersley number α, the amplitude of the pressure pulsation ϵ, the Schmidt number S, the aspect ratio λ, the reaction parameter β and the dispersion time t.

For an oscillatory current $u = u_1(r, t)$ and when $\epsilon = 1$, $\mathrm{Pe} = S = 10^3$, the variation of D_a with respect to time is depicted for different values of β in Fig. 3a,b for $\alpha = 0{\cdot}5$ and $\lambda = 0{\cdot}1$; in Fig. 3c,d for $\alpha = 2{\cdot}0$ and $\lambda = 0{\cdot}1$; and for different values of λ in Fig. 3e,f for $\alpha = 1{\cdot}0$ and

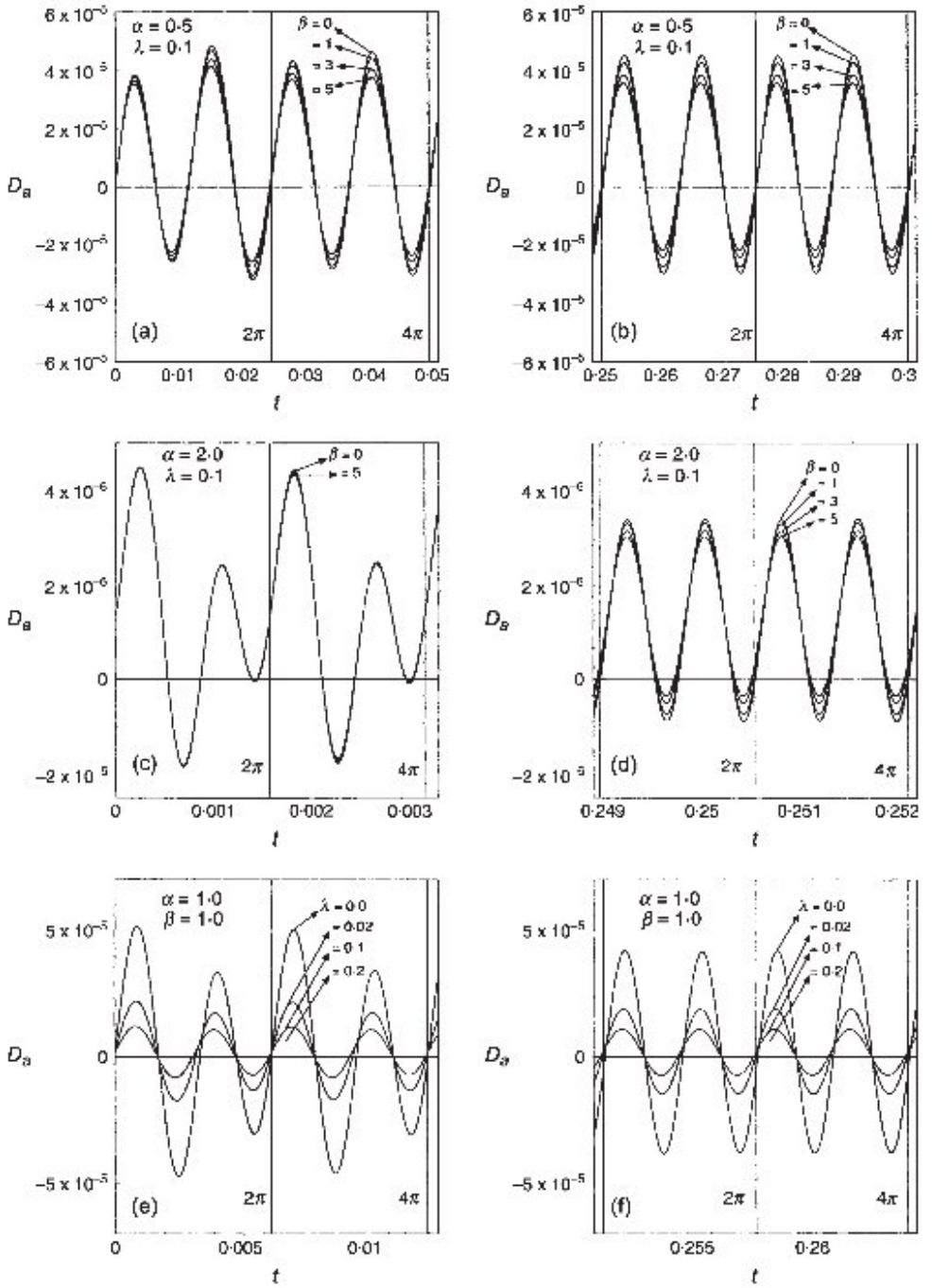

Fig. 3 Temporal variation of the dispersion coefficient D_a for periodic flow with zero mean for various values of β and λ: (a), (c), (e) for small time and (b), (d), (f) for large time when $\epsilon = 1$, $\mathrm{Pe} = S = 10^3$

$\beta = 1{\cdot}0$. It is seen from the figures that for periodic flow with zero mean the dispersion coefficient D_a changes cyclically with a double-frequency period and it reaches a non-transient state after a certain critical time t_c, which is related to the cross-sectional mixing time a^2/D. In the case of low frequency $\alpha = 0{\cdot}5$, the amplitudes of oscillation of D_a during the first and second half of the period of oscillation are almost equal, whereas for large frequency $\alpha = 2{\cdot}0$, the amplitude of D_a is more significant during the first half of the period than the second one (Mazumder and Das (**16**)). It is also observed that when the frequency parameter α is small, D_a reaches a non-transient state earlier than in the case of high frequency. However, this dispersion process completely stabilizes after a certain time and then the solute disperses at a fairly uniform rate with oscillation. Further, the dispersion coefficient D_a for a given frequency parameter α decreases with increase in the reaction parameter β. It is also clear from the figures that the dispersion coefficient D_a reduces with increase of the Womersley number α. This is because increase of the Womersley number reduces the flow within the annular region, hence the reduction of D_a. From Fig. 3e,f, it is interesting to note that in an annular pipe ($\lambda = 0{\cdot}02$), the dispersion coefficient D_a suddenly, drops compared with its value for a tube ($\lambda = 0$). Also it is seen that as the aspect ratio λ increases the dispersion coefficient D_a decreases, that is, decrease of the annular gap size inhibits the dispersion process. This can be explained by the fact that an increase of λ leads to a decrease of the flow within the annular region which causes a lower dispersion rate. The temporal variation of D_a due to the combined effects of a steady and periodic current for $\epsilon = 1$, $\mathrm{Pe} = S = 10^3$ have been plotted in Fig. 4a,b for various values of λ and $\alpha = \beta = 1$; and in Fig. 5a,b for various values of β and $\alpha = 0{\cdot}5$, $\lambda = 0{\cdot}1$. In all cases, D_a varies with a single period of oscillation and in terms of its magnitude, the amplitude of oscillation increases initially up to a certain time, and then becomes stable for a long time, which implies that the dispersion coefficient D_a for the steady flow plays a more significant role than that for the periodic flow. It is also observed from Fig. 5a,b that for fixed Womersley number $\alpha = 0{\cdot}5$ and $\lambda = 0{\cdot}1$, an increase of the reaction parameter at the wall leads to a decrease of the dispersion

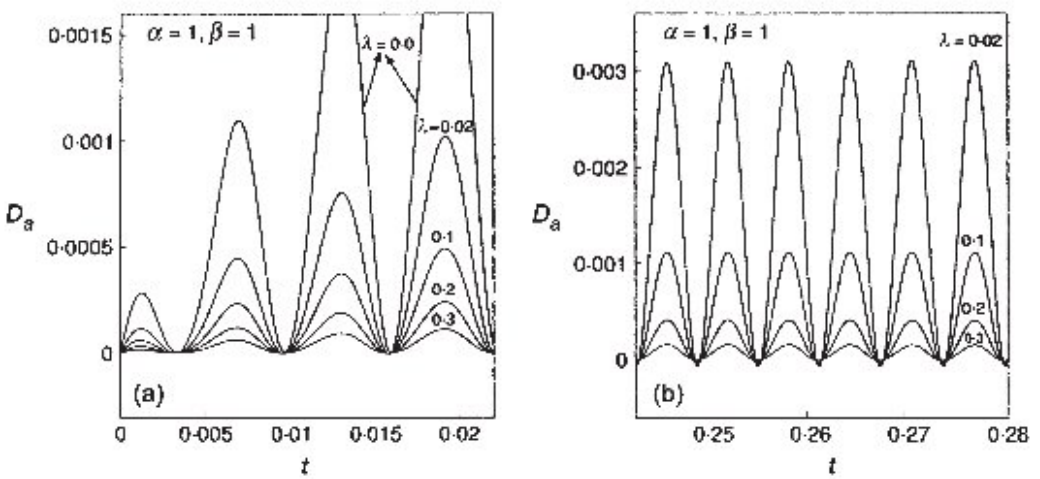

Fig. 4 Dispersion coefficient D_a for periodic flow with non-zero mean for different λ: (a) for small time and (b) for large time when $\epsilon = 1$, $\mathrm{Pe} = S = 10^3$

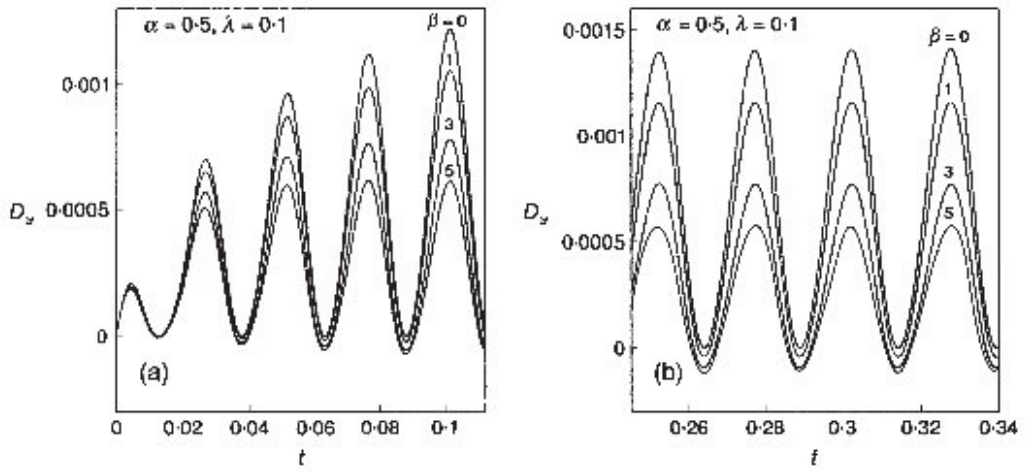

Fig. 5 Variation of the dispersion coefficient D_a for periodic flow with non-zero mean for various values of β: (a) for small time and (b) for large time when $\epsilon = 1$, $\mathrm{Pe} = S = 10^3$

coefficient D_a. Thus, one would expect that an increase in β leads to an increasing number of moles of reactive solute undergoing chemical reaction or absorption, and hence there is a drop in D_a. From Figs 4a,b and 5a,b it is clearly observed that, for fixed α, β and λ, the dispersion coefficient D_a no longer has the double-frequency period and it is always positive unlike the oscillatory flow. Figure 6 shows the variation of the coefficient of skewness with time for periodic flow with zero mean when $\epsilon = 1$, $\mathrm{Pe} = S = 10^3$, $\alpha = 0{\cdot}5$ and for various values of β and λ. It is observed that the skewness in the periodic flow changes cyclically with a single-frequency period and it decreases with dispersion time t. The effect of the reaction parameter β on the skewness coefficient is not significant (see Fig. 6a,b) with respect to the dispersion time t, but the influence of the aspect ratio λ on λ_3 is significant and is shown in Fig. 6c,d. It is observed that as λ increases the amplitude of oscillation of λ_3 decreases, which shows that with increase of the aspect ratio, the concentration of solute tends to a Gaussian distribution at large time.

The variation of λ_3 due to the shear effect of a periodic current with non-zero mean has been plotted in Fig. 7a,b for $\epsilon = 1$, $\mathrm{Pe} = S = 10^3$ and for various values of β and λ. It is seen from Fig. 7a that the skewness initially decreases with time and then increases; and moves asymptotically to a constant value after a certain time. Also it is observed that for small β the distribution is asymmetric, but when $\beta(= 5)$ is large, it has a tendency to reach a symmetric form at large time. A similar result is also observed in Fig. 7b—the magnitude of the skewness of the distribution increases up to a certain value with increase of λ, and then decreases with further increase of λ as the distribution moves towards a Gaussian distribution. The temporal variation of the kurtosis λ_4 due to the shear effect of periodic flow with zero mean is depicted in Fig. 8 for $\epsilon = 1$, $\mathrm{Pe} = S = 10^3$ and for various values of β and λ. It is seen from Fig. 8a,b that for $\alpha = 0{\cdot}5$ and $\lambda = 0{\cdot}1$, the effect of the reaction parameter β on the kurtosis is significant with the dispersion time t except at very small time. This is because at very small time the solute does not interact with the reaction at the pipe boundary and as β increases it is observed that the amplitude of the kurtosis increases, which leads to decrease of the peak of the mean concentration distribution. In Fig. 8c,d it is observed that the kurtosis moves

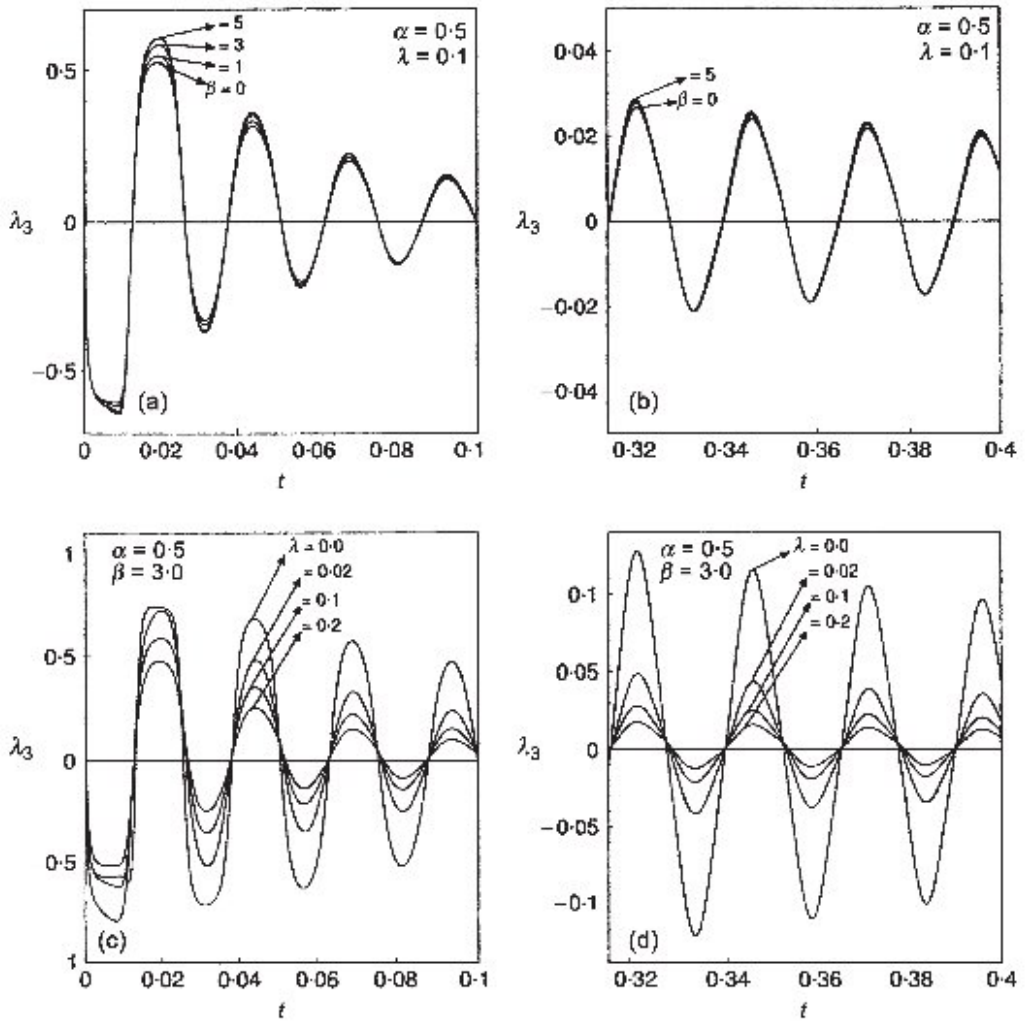

Fig. 6 Skewness (λ_3) of the distribution for periodic flow with zero mean for different β and λ: (a), (c) for small time and (b), (d) for large time, when $\epsilon = 1$, $\mathrm{Pe} = S = 10^3$

cyclically with the dispersion time t and it is interesting to note that at large time the kurtosis tends to zero as λ increases, which implies that the distribution approaches the Gaussian distribution.

Using the central moments $\mu_2, \lambda_3, \lambda_4$ of the distribution, it is possible to compute the mean axial concentration distribution $C_m(t, z)$ of tracers within the annular region with the help of a Hermite polynomial representation for non-Gaussian curves (Chatwin (**28**) and Güven *et al.* (**29**)):

$$C_m(t, z) = M_0(t)e^{-x^2} \sum_{n=0}^{\infty} a_n(t)H_n(x), \tag{22}$$

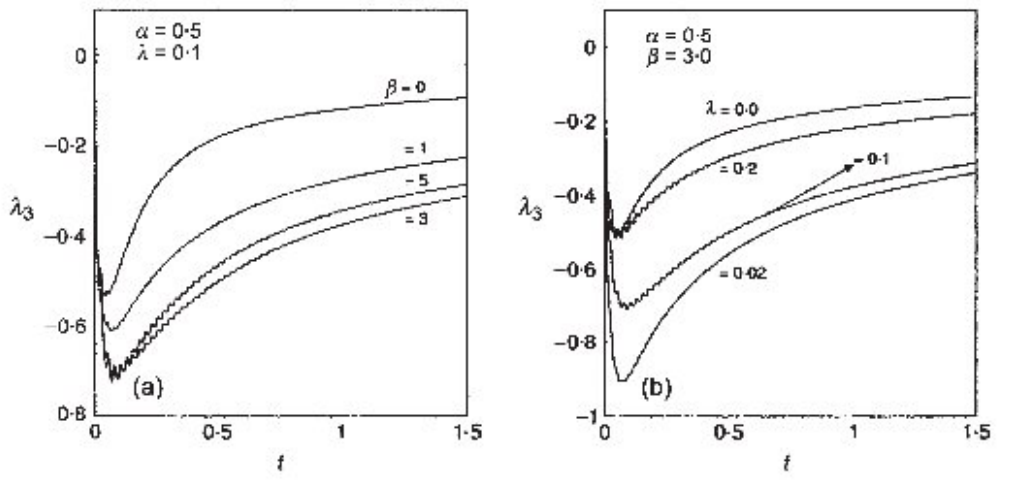

Fig. 7 Temporal variation of the skewness (λ_3) of the distribution for periodic flow with non-zero mean: (a) for different β and (b) for different λ when $\epsilon = 1$, $\mathrm{Pe} = S = 10^3$

where $x = (z - \mu_g)/(2\mu_2)^{1/2}$, $\mu_g = M_1/M_0$ and H_i are the Hermite polynomials, satisfying the recurrence relation

$$H_{i+1}(x) = 2x\,H_i(x) - 2i\,H_{i-1}(x), \quad i = 0, 1, 2, \ldots \tag{23}$$

with $H_0(x) = 1$. The coefficients a_i are

$$a_0 = 1/(2\pi\mu_2)^{1/2}, \quad a_1 = a_2 = 0, \quad a_3 = 2^{1/2}a_0\lambda_3/24, \quad a_4 = a_0\lambda_4/96.$$

The variation of the mean concentration distribution $C_m(t, z)$ is presented in Fig. 9 as a function of the axial distance $(z - \mu_g)$ for periodic flow with zero mean through an annular pipe for $\epsilon = 1$, $\mathrm{Pe} = S = 10^3$. It is seen from Fig. 9a (with $\alpha = 0{\cdot}5$, $\beta = 3{\cdot}0$, $\lambda = 0{\cdot}2$ fixed) that as the dispersion time t increases, the peak of the distribution decreases and tends to become flat (solid line). It is also clear from the figure (dotted line) that for $\alpha = 3{\cdot}0$, $t = 0{\cdot}2$, $\lambda = 0{\cdot}2$, an increase of the reaction parameter β leads to a depletion of the amount of reactive material, and therefore the peak of the mean concentration distribution gradually decreases. Figure 9b shows that for $t = 0{\cdot}2$, $\lambda = 0{\cdot}1$, $\beta = 1{\cdot}0$, the peak of the axial distribution of mean concentration increases with increase in the Womersley number α. It is interesting to note from the figure that for low frequency $\alpha(= 0{\cdot}5)$, an increase of λ has a significant effect on the distribution, whereas at high frequency α this effect diminishes. Therefore, as α increases, the effect of λ tends to become insignificant in the concentration distribution. This may be explained by the fact that with increase in both λ and α the dispersion of tracer molecules decreases, and hence tracer materials concentrate in a smaller region in the axial direction. From Fig. 9c it is observed that, for two different frequencies $\alpha = 0{\cdot}5$ (dotted lines) and $\alpha = 3{\cdot}0$ (solid lines) with $\beta = 0$, $t = 0{\cdot}2$, as λ increases from 0 (pipe Poiseuille flow) to 0.4 (annular flow) the peak of the distribution increases and the axial distance gradually decreases. It is clearly seen that for $\alpha = 3$ and $\beta = 0$ the effect of aspect ratio λ on the mean concentration distribution is insignificant compared with that for low frequency $\alpha = 0{\cdot}5$ and $\beta = 0$.

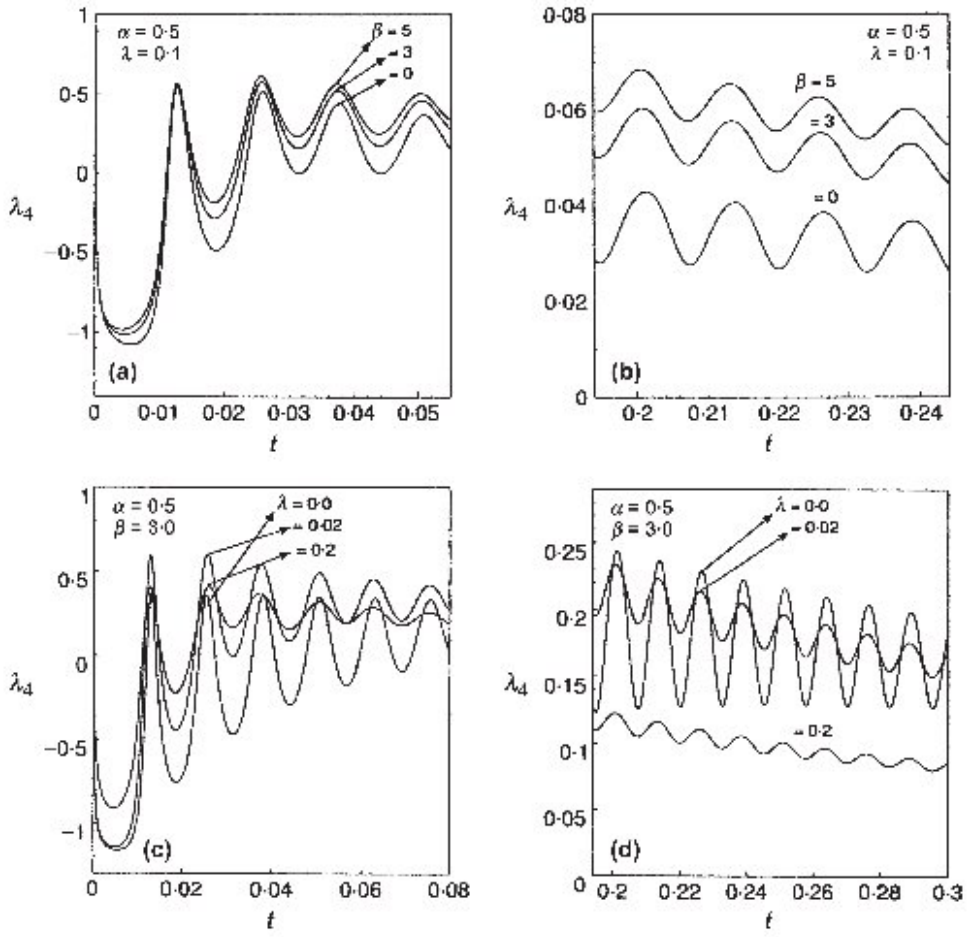

Fig. 8 Temporal variation of the kurtosis (λ_4) of the distribution for periodic flow with zero mean for different β and λ: (a), (c) for small time and (b), (d) for large time, when $\epsilon = 1$, $\mathrm{Pe} = S = 10^3$

Finally, for comparison, the profiles of $C_m(t, z)$ along the axial direction are plotted in Fig. 10a,b for periodic flow with non-zero mean for $\epsilon = 1$, $\mathrm{Pe} = S = 10^3$. Figure 10a for $\alpha = 0{\cdot}5$, $\beta = 3{\cdot}0$, $\lambda = 0{\cdot}2$ (solid line) shows that as the dispersion time t increases, the peak of the distribution becomes flatter and moves to a Gaussian distribution; and for $\alpha = 0{\cdot}5$, $t = 0{\cdot}2$, $\lambda = 0{\cdot}2$ (dotted line) it is observed that as the reaction parameter β increases, the peak of the distribution gradually decreases. Figure 10b for $\alpha = 0{\cdot}5$, $t = 0{\cdot}2$, $\beta = 3{\cdot}0$, shows that as λ increases from 0 (pipe Poiseuille flow) to 0·4 (annular flow) the peak of the distribution increases and the asymmetric distribution of mean axial concentration moves towards a symmetrical one. It is worthwhile to note that the role of the Womersley number α in the mean concentration distribution for periodic flow with a non-zero mean is less significant compared with that for periodic flow with zero mean.

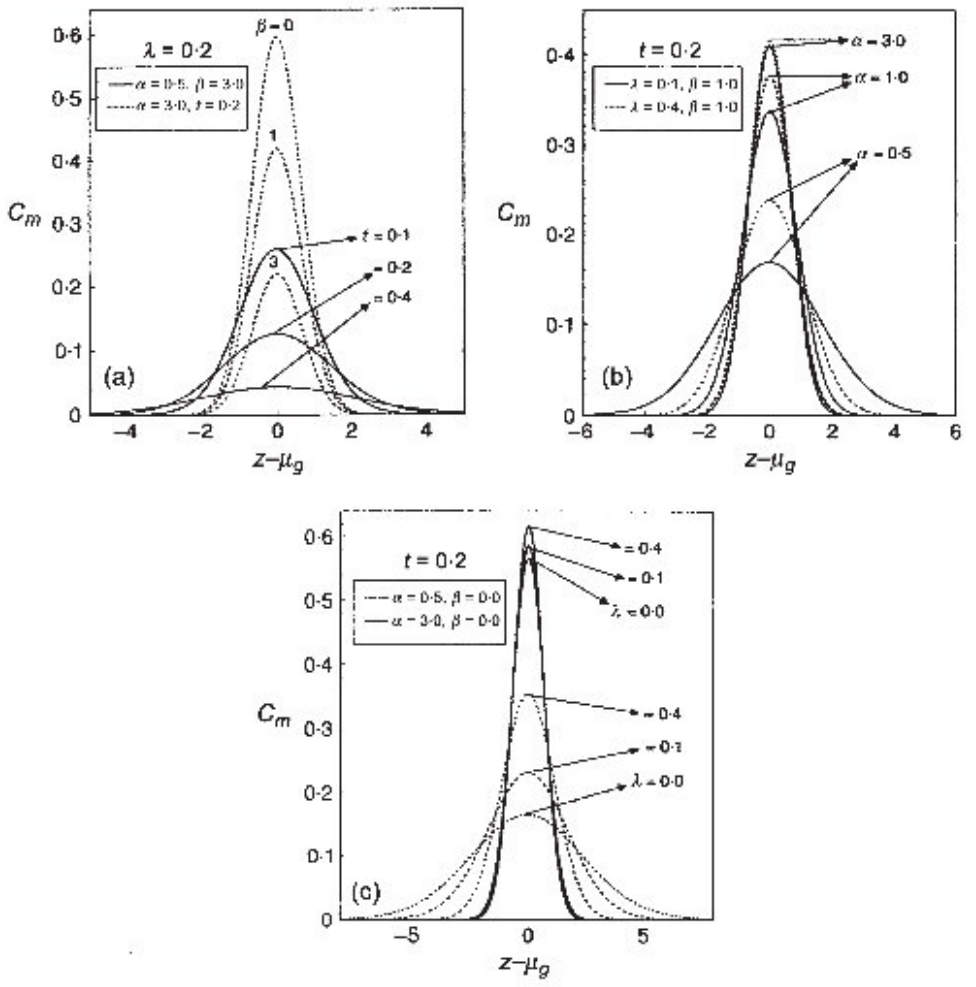

Fig. 9 Axial distribution of concentration $C_m(t, z)$ for periodic flow with zero mean for $\epsilon = 1$, $\mathrm{Pe} = S = 10^3$: (a) for different dispersion times t (solid lines) and for different β (dotted lines); (b) for different α and $\lambda = 0.1$ (solid lines), $\lambda = 0{\cdot}4$ (dotted lines); (c) for different λ and $\alpha = 0{\cdot}5$ (dotted lines), $\alpha = 3{\cdot}0$ (solid lines)

5. Applications to a catheterized artery

The results discussed in section 4 are important in understanding the dispersion process through a catheterized artery with a reactive arterial wall. The tube of radius a can be considered as a blood vessel and the insertion of another tube of radius b (that is, the catheter) into the blood vessel causes the formation of an annular region between the catheter wall and the arterial wall. The parameter λ, the ratio of the catheter radius b to the arterial radius a is varied from 0·02 to 0·4 to analyse the effect of the catheter size on dispersion. The catheterization increases the frictional resistance to flow

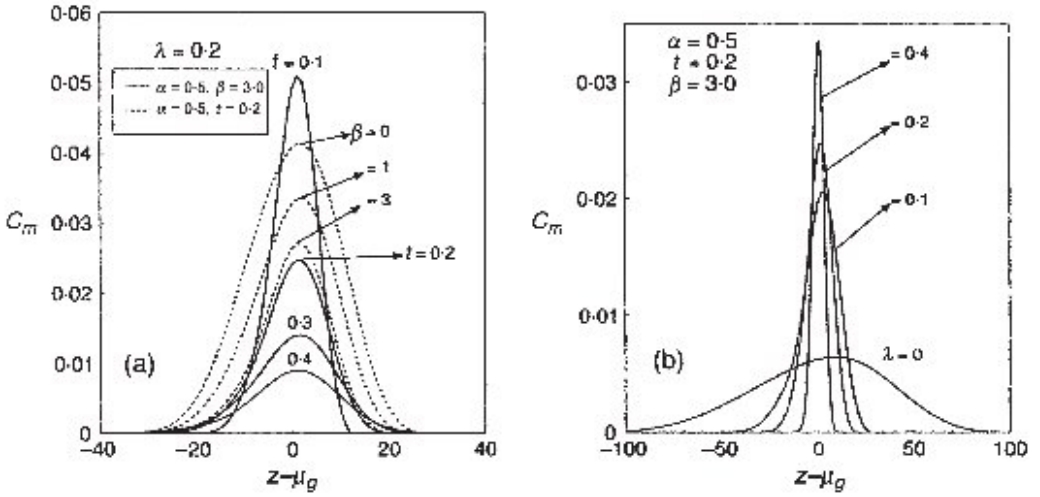

Fig. 10 Mean concentration distribution $C_m(t, z)$ for periodic flow with non-zero mean for $\epsilon = 1$, $\mathrm{Pe} = S = 10^3$: (a) for different dispersion times t (solid lines) and for different β (dotted lines) and (b) for different λ

through the artery and hence alters the flow field owing to changes of haemodynamic conditions in the artery. In order to make an accurate pressure reading in an annular region, it is essential to understand the catheter-induced error. The results of the present problem may provide a correction for catheter insertion in the light of the behaviour of the longitudinal dispersion coefficient and the mean concentration distribution of tracers. To relate the present study with arterial blood flow, the Schmidt number S is restricted to the order of 10^3 for diffusion in blood (Waters (**30**)). Figures 3, 4 and 5 describe the temporal variation of the dispersion coefficient D_a for different values of the frequency parameter α, absorption parameter β and catheter size λ for $\mathrm{Pe} = S = 10^3$ and $\epsilon = 1$. It is seen that increase of the Womersley parameter, absorption parameter or catheter size inhibits the dispersion process (Sarkar (**31**)). It is observed that when a catheter ($\lambda = 0.02$) is introduced into an artery, the dispersion coefficient D_a suddenly drops in comparison to that of an un-catheterized ($\lambda = 0$) artery. From Figs 9 and 10 showing the mean concentration distribution of tracer molecules, it is seen that the peak of the distribution increases with increase of both the catheter size (Sarkar (**31**)) and the Womersley number, and it decreases with increase of the dispersion time t and boundary absorption β. It is clearly observed that the insertion of a catheter (Fig. 9b) in the artery leads to an insignificant effect for high Womersley number α.

6. Conclusions

We have focused our attention on the dispersion process of tracer molecules in a pulsatile flow and, for comparison, in a periodic flow with non-zero mean, through a pipe of annular cross-section with a reactive wall. We have compared some specific results due to the shear effect with particular emphasis on the role played by the combination of reaction at the outer wall of the annular pipe and the aspect ratio λ. The apparent dispersion coefficient D_a is a function of the Womersley number α,

the Schmidt number S, the amplitude of the pressure pulsation ϵ, the aspect ratio λ, the reaction parameter β and the dispersion time t. It is observed that the dispersion process is inhibited by an increase of the Womersley number, aspect ratio or reaction parameter for periodic flows with or without a non-zero mean. However, the dispersion coefficient D_a for a periodic flow with non-zero mean no longer has the double frequency period compared with the dispersion coefficient D_a for a periodic flow with zero mean. The effect of aspect ratio λ, reaction parameter β and frequency parameter α on the mean concentration distribution has been studied for periodic flows with and without a non-zero mean. It is observed that for low frequency an increase of λ has a significant effect on the mean concentration distribution of tracers but for large frequency the effect of λ diminishes. It is also seen that an increase of λ and the Womersley number α leads to a decrease of D_a and hence the tracer molecules concentrate in the annular region, and are depleted due to boundary absorption. Results of the present mathematical model are analysed in the context of a catheterized artery with a reactive arterial wall in section 5.

Acknowledgements

The second author thanks the CSIR, India, for financial support in pursuing this work. The authors would also like to express sincere thanks to three referees for providing suggestions for improvement of the paper.

References

1. G. I. Taylor, *Proc. R. Soc.* A **219** (1953) 186–203.
2. R. Aris, *ibid.* A **235** (1956) 67–77.
3. R. Aris, *ibid.* A **259** (1960) 370–376.
4. E. J. Watson, *J. Fluid Mech.* **133** (1983) 233–244.
5. J. B. Grotberg, *ibid.* **141** (1984) 249–264.
6. D. P. Gaver and J. B. Grotberg, *ibid.* **172** (1986) 47–61.
7. A. R. Rao and K. S. Deshikachar, *Z. Angew. Math. Mech.* **67** (1987) 189–195.
8. W. N. Gill and R. Sankarasubramanian, *Proc. R. Soc.* A **316** (1970) 341–350.
9. T. J. Pedley and R. D. Kamm, *J. Fluid Mech.* **193** (1988) 347–367.
10. P. C. Chatwin, *ibid.* **71** (1975) 513–527.
11. C. F. Jimenez and P. J. Sullivan, *ibid.* **142** (1984) 57–77.
12. A. Mukherjee and B. S. Mazumder, *Acta Mech.* **74** (1988) 107–122.
13. P. E. Hydon and T. J. Pedley, *J. Fluid Mech.* **249** (1993) 535–555.
14. R. Smith, *ibid.* **134** (1983) 161–177.
15. A. Purnama, *ibid.* **195** (1988) 393–412.
16. B. S. Mazumder and S. K. Das, *ibid.* **239** (1992) 523–549.
17. Y. Jiang and J. B. Grotberg, *J. Biomech. Engng* **115** (1993) 424–431.
18. G. Jayaraman, T. J. Pedley and A. Goyal, *Q. Jl Mech. Appl. Math.* **51** (1998) 577–598.
19. L. H. Back, E. Y. Kwack and M. R. Back, *J. Biomech. Engng* **118** (1996) 83–89.
20. M. R. Back, E. Y. White and L. H. Back, *Angiology* **48** (1997) 99–109.
21. G. Jayaraman and K. Tiwari, *Med. Biol. Engng Comput.* **33** (1995) 1–6.
22. R. K. Dash, G. Jayaraman and K. N. Mehta, *J. Biomech.* **29** (1996) 917–930.
23. A. Sarkar and G. Jayaraman, *Phys. Fluids* **13** (2001) 2901–2911.
24. S. Tsangaris and N. Athanassiadis, *Z. Angew. Math. Mech.* **65** (1985) T252–T254.

25. M. Abramowitz and I. A. Stegun, *Handbook of Mathematical Functions* (Dover, New York 1965).
26. D. A. Anderson, J. C. Tanehill and R. H. Pletcher, *Computational Fluid Mechanics and Heat Transfer* (Hemisphere, New York 1984).
27. N. G. Barton, *J. Fluid Mech.* **126** (1983) 205–218.
28. P. C. Chatwin, *ibid.* **43** (1970) 321–352.
29. O. Güven, F. J. Molz and J. G. Melville, *Water Resour. Res.* **29** (1984) 1337–1354.
30. S. L. Waters, *J. Fluid Mech.* **433** (2001) 193–208.
31. A. Sarkar, Flow and dispersion in a catheterized artery: a theoretical model, Ph.D. Thesis, 1999.